

# MECHANICAL RESPONSE ANISOTROPY IN HOT-PRESSED SILICON CARBIDE<sup>1</sup>

A. A. Wereszczak,<sup>1</sup> D. J. Vuono,<sup>2</sup> K. P. Bortle,<sup>2</sup> P. J. Ritt,<sup>2</sup> J. J. Swab,<sup>3</sup> and J. Campbell<sup>3</sup>

<sup>1</sup> Oak Ridge National Laboratory, Oak Ridge, TN 37831.

<sup>2</sup> ORISE, Oak Ridge National Laboratory, Oak Ridge, TN 37831.

<sup>3</sup> US Army Research Laboratory, Aberdeen Proving Ground, MD 21005.

## ABSTRACT

Property anisotropy can exist in sintered ceramics and composites formed by pressure-assistance. Being that hot-pressed silicon carbide (SiC) is a utilized armor ceramic, and its fracture and damage multiaxially occurs in a ballistic impact, interest exists to measure the quasi-static mechanical (fracture and indentation) responses as a function of orientation to identify anisotropy. Flexure strength, fracture toughness, Knoop hardness, and spherical indentation were studied as a function of orientation with respect to the pressing axis in a 40-mm-thick hot-pressed SiC tile. Flexure strength and fracture toughness were ~ 25% and 10% lower, respectively, in the plane perpendicular to the pressing axis while hardness was isotropic and the responses from spherical indentation were different but inconclusive.

## INTRODUCTION

The fracture and damage chronologies in an armor ceramic undergoing a ballistic event is complex and multiaxial. While the understanding of their damage evolutions have certainly advanced, one important and taken-for-granted assumption in respect to their predicted response is that properties of the ceramic are isotropic. This means that fracture (tensile-, compression-, and shear-induced) and confined high-pressure-induced processes occur independent of material processing orientation.

Uniaxial pressure-assisted sintering of ceramics and composites tends to promote a transverse isotropic microstructure habit that can cause anisotropic properties. This is particularly true as the thickness of a processed component increases whereby the history of shear-transfer and compaction among the powder constituents is less efficient before sintering commences.

Lange reported such anisotropy in Si<sub>3</sub>N<sub>4</sub> [1], and Weston went on to quantify it [2], finding that members taken along an axis parallel to the hot pressing axis had only a fraction of the strength found in traditionally harvested members. Similar results were found in alumina-based materials [3]. In each of these studies, the anisotropies were attributed to preferential alignment of elongated grains during hot-pressing. Additionally the uniaxial pressing action can lead to density variations which can be magnified as component thickness increases. Takashi et al., showed that forces are not evenly transmitted throughout the material during pressing and

---

<sup>1</sup> As the primary authors are not Government employees, this document was only reviewed for export controls, and improper Army association or emblem usage considerations. All other legal considerations are the responsibility of the author and their employers.

## Report Documentation Page

*Form Approved*  
*OMB No. 0704-0188*

Public reporting burden for the collection of information is estimated to average 1 hour per response, including the time for reviewing instructions, searching existing data sources, gathering and maintaining the data needed, and completing and reviewing the collection of information. Send comments regarding this burden estimate or any other aspect of this collection of information, including suggestions for reducing this burden, to Washington Headquarters Services, Directorate for Information Operations and Reports, 1215 Jefferson Davis Highway, Suite 1204, Arlington VA 22202-4302. Respondents should be aware that notwithstanding any other provision of law, no person shall be subject to a penalty for failing to comply with a collection of information if it does not display a currently valid OMB control number.

1. REPORT DATE <b>07 JAN 2013</b>	2. REPORT TYPE <b>Journal Article</b>	3. DATES COVERED <b>08-03-2012 to 28-12-2012</b>			
4. TITLE AND SUBTITLE <b>MECHANICAL RESPONSE ANISOTROPY IN HOT-PRESSED SILICON CARBIDE</b>		5a. CONTRACT NUMBER			
		5b. GRANT NUMBER			
		5c. PROGRAM ELEMENT NUMBER			
6. AUTHOR(S) <b>A Wereszczak; D Vuono; K Vuono; P Ritt; J Swab</b>		5d. PROJECT NUMBER			
		5e. TASK NUMBER			
		5f. WORK UNIT NUMBER			
7. PERFORMING ORGANIZATION NAME(S) AND ADDRESS(ES) <b>Oak Ridge National Laboratory, 4500 X10 Area, Oak Ridge, TN, 37831</b>		8. PERFORMING ORGANIZATION REPORT NUMBER <b>; #23590</b>			
9. SPONSORING/MONITORING AGENCY NAME(S) AND ADDRESS(ES) <b>U.S. Army TARDEC, 6501 East Eleven Mile Rd, Warren, Mi, 48397-5000</b>		10. SPONSOR/MONITOR'S ACRONYM(S) <b>TARDEC</b>			
		11. SPONSOR/MONITOR'S REPORT NUMBER(S) <b>#23590</b>			
12. DISTRIBUTION/AVAILABILITY STATEMENT <b>Approved for public release; distribution unlimited</b>					
13. SUPPLEMENTARY NOTES					
14. ABSTRACT <b>Property anisotropy can exist in sintered ceramics and composites formed by pressure-assistance. Being that hot-pressed silicon carbide (SiC) is a utilized armor ceramic, and its fracture and damage multiaxially occurs in a ballistic impact, interest exists to measure the quasi-static mechanical (fracture and indentation) responses as a function of orientation to identify anisotropy. Flexure strength, fracture toughness, Knoop hardness, and spherical indentation were studied as a function of orientation with respect to the pressing axis in a 40-mm-thick hotpressed SiC tile. Flexure strength and fracture toughness were ~ 25% and 10% lower, respectively, in the plane perpendicular to the pressing axis while hardness was isotropic and the responses from spherical indentation were different but inconclusive.</b>					
15. SUBJECT TERMS					
16. SECURITY CLASSIFICATION OF:			17. LIMITATION OF ABSTRACT <b>Public Release</b>	18. NUMBER OF PAGES <b>10</b>	19a. NAME OF RESPONSIBLE PERSON
a. REPORT <b>unclassified</b>	b. ABSTRACT <b>unclassified</b>	c. THIS PAGE <b>unclassified</b>			

measured that, under certain pressing conditions, density could vary by up to almost 10 percent [4]. That observation was found in a uniaxial dry pressed green body, but the factors responsible for the effect are found in hot pressed systems as well.

Hot-pressed SiC is a common armor ceramic, thus interest exists in this study to conduct various quasi-static mechanical (fracture and indentation) responses as a function of orientation to explore any anisotropic response.

## MATERIAL AND EXPERIMENTAL DESCRIPTION

### *Material*

The material evaluated in this study was a hot-pressed silicon carbide designated by its manufacturer (BAE Systems, Advanced Ceramics Division, Vista, CA) as SiC-N. The density, elastic modulus and Poisson's ratio of this material were previously measured [5] and are shown in Table I. A block of this material, dimensions of 100 x100 x 40 mm thick, was sectioned into coupons of three orientations with respect to pressing direction, as shown in Fig. 1. Z is defined as the direction parallel to the press direction, while two orthogonal R directions are perpendicular. These orientations were chosen to create three unique fracture strength and fracture toughness ( $K_{Ic}$ ) combinations. Table II shows the tensile stress direction and fracture plane as well as the  $K_{Ic}$  fracture plane and direction for each orientation. Microstructures of each orientation are shown in Fig. 2. Orientation 1 represents conventionally harvested coupons, such as those used to calculate the physical properties shown in Table I [5]. All coupons had a 4 x 2 mm cross-section, but each orientation was given a different length as a means of axis differentiation.

Table I. Density, elastic modulus, and Poisson's ratio of the SiC-N [5].  $\pm$  values are one standard deviation.

<b>SiC grade</b>	<b>Density (g/cm<sup>3</sup>)</b>	<b>Elastic Modulus (GPa)</b>	<b>Poisson's Ratio</b>	<b>Average Grain Size (<math>\mu</math>m)</b>
SiC-N	3.21 $\pm$ 0.01	454 $\pm$ 4	0.171 $\pm$ 0.012	3.25 $\pm$ 2.10

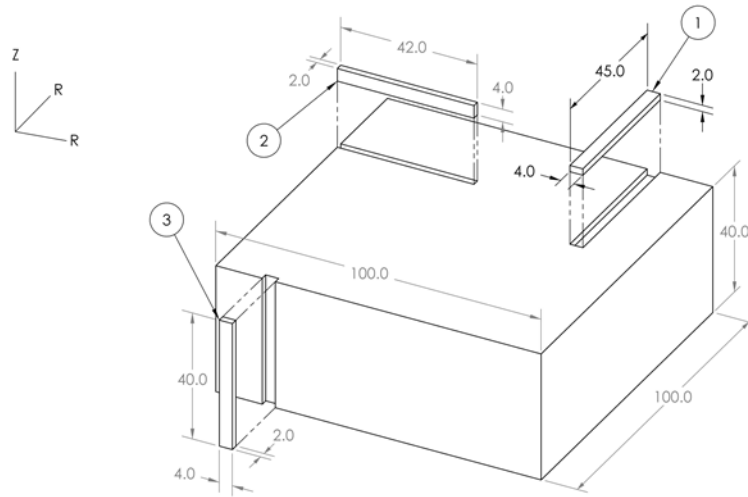
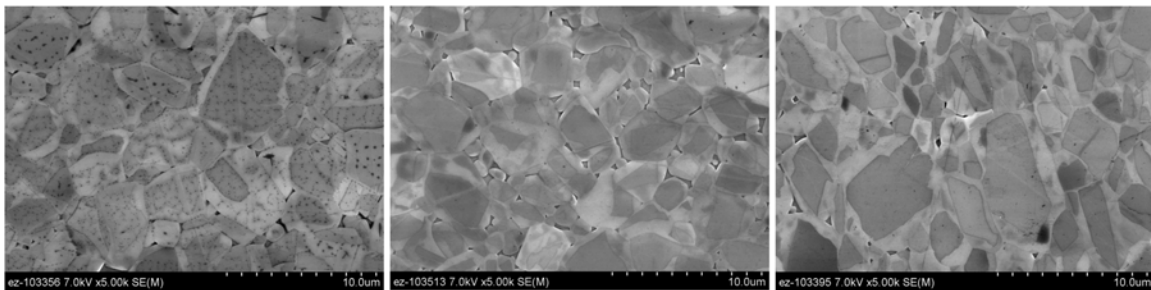


Figure 1. Schematic drawing of tile dimensions (units in mm) with respect to the three investigated orientations. Hot-pressing direction is parallel to the Z-axis. Cross-sectional dimensions were identical in all orientations; however, lengths were purposely different to provide orientation traceability.

Table II. Tensile stress direction and fracture plane,  $K_{Ic}$  fracture direction and plane for three unique coupon orientations.

Orientation	Tensile Stress Direction	Tensile Stress Fracture Plane	$K_{Ic}$ Fracture Direction	$K_{Ic}$ Fracture Plane
1	R	R-Z	R	R-Z
2	R	R-Z	Z	R-Z
3	Z	R-R	R	R-R



10  $\mu$ m

Figure 2. Microstructures of (left to right) orientations 1, 2, and 3.

### Flexure Strength

Flexure strength testing was performed to determine whether crack initialization resistance in the R-R plane of the material varied from that of the R-Z plane. Forty-five test coupons of each orientation were identically prepared and longitudinally ground per ASTM C1161 [6]. Coupons were tested according to the methods in ASTM C1161. Span size was chosen relative to specimen cross-sectional size so to produce valid beam bend testing and gage section failure. The strength ( $S$ ) for each coupon was calculated using

$$S = \frac{3P(L_o - L_i)}{2bh^2}$$

where  $P$  is failure force,  $L_o$  (= 31.75 mm) and  $L_i$  (= 15.88 mm) are outer and inner span sizes, and  $b$  and  $h$  are specimen width and height, respectively. Commercial statistical software was used to fit calculated flexure strengths to a two-parameter Weibull distribution using maximum likelihood estimation.

### Fracture Toughness

An additional 30 coupons were machined to the geometry shown in Fig. 3 to observe crack propagation behavior variation in the material due to orientation. Fracture toughness of the three orientations was measured using chevron notch geometry from ASTM C1421 [7]. Ten coupons of each orientation were tested in three-point flexure using a 31.75 mm span. A displacement rate of 60  $\mu\text{m}/\text{min}$  was used to induce stable crack propagation in all tests. After failure, the chevron notch dimensions were measured to calculate the  $K_{Ic}$  of each coupon based upon ASTM C1421. Average  $K_{Ic}$  values for each orientation were determined.

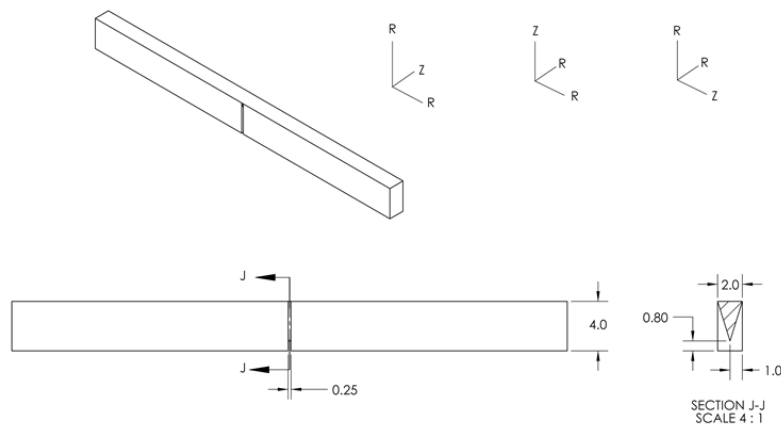


Figure 3. Schematic drawing of fracture toughness coupon chevron notch geometry with corresponding coupon axes - from left to right, axes for orientation 1, 2 and 3. Units are in mm.

### *Knoop Indentation*

A micro-hardness tester was used to measure Knoop hardness following the indentation method described in ASTM C1326 [8]. To confirm the calibration of the instrument, five 19.6 N Knoop indents were produced in the National Institute of Standards and Technology's (NIST) standard reference material SRM 2830 [9], and their average hardness was confirmed to vary <1% from the certified average value. Twenty Knoop indentations were generated in one coupon of each of the three orientations on the coupon's broadest face. Ten of these indents were aligned parallel to the bend bar axis and ten were perpendicularly aligned. A load of 1 kgf (9.8N) was used to produce mostly (ideally all) plastic deformation with minimal fracture. Lengths of each indentation were then measured, and used to calculate the Knoop hardness ( $HK$ ) in GPa using

$$HK = 0.014229 \left( \frac{P}{d^2} \right)$$

where  $P$  is indentation force, and  $d$  is the length of the long diagonal of the Knoop indent. Additionally, several indents from each specimen (three of each alignment) were viewed using a scanning electron microscope to examine cracking extending from the tips of the indents.

### *Spherical Indentation*

Spherical indentation was performed using a 500- $\mu\text{m}$ -diameter spherical diamond indenter on the same polished coupons used for hardness testing. Five indents were made on each coupon and a maximum force of 20 N was used each time. A displacement rate of 10  $\mu\text{m}/\text{min}$  was used. Force ( $F$ ) and indentation depth ( $U$ ) data were recorded. Semi-quantitative analysis was performed based upon the maximum indenter depth of penetration (IDOP) and residual depth of indent of each indentation.

## RESULTS AND DISCUSSION

### *Tensile Fracture Response (Flexure Strength and Fracture Toughness)*

Weibull strength distributions for each orientation are portrayed in Figs. 4 and 5. The characteristic strength ( $\sigma_\theta$ ) and Weibull modulus ( $m$ ) for each orientation with  $\pm 95\%$  confidence bands shown in parenthesis are all included in Fig. 4. Orientation 3 had the lowest characteristic strength of the three orientations by about 25%. This is a statistical trend seen in other hot-pressed materials [2]. Nearly a third of the failures of orientation 3 occurred at stresses lower than the weakest specimens of orientations 1 and 2. The significant difference of orientation 3's strength distribution is also illustrated in Fig. 5. Directionality of fracture within the R-R plane has no significant effect on flexure strength, as there is no significant difference found between the strengths of orientations 1 and 2. Consistent with strength, fractography showed no conclusive differences among orientations 1 and 2.

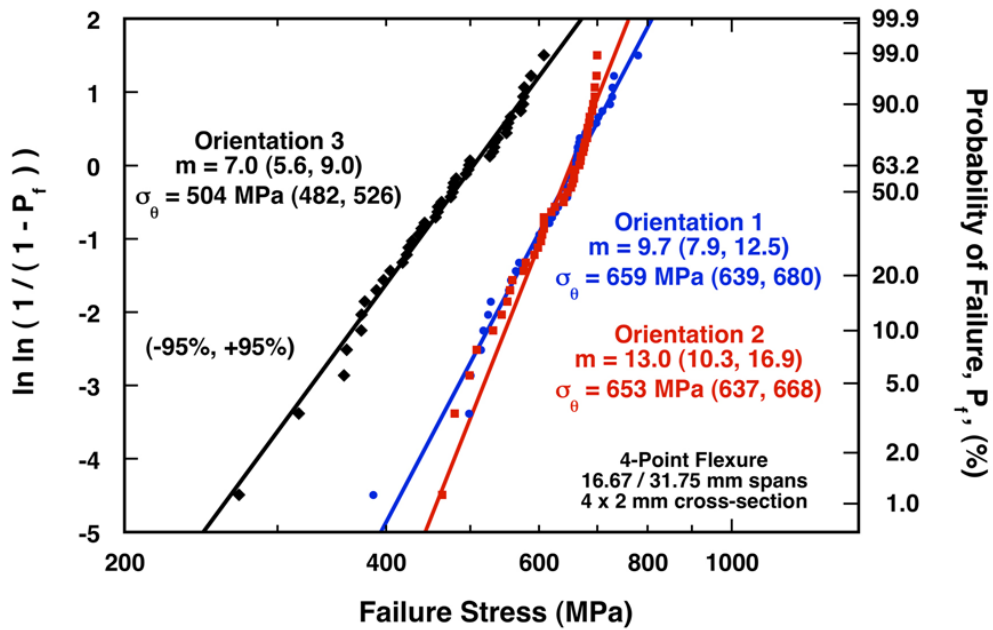


Figure 4. Weibull flexure strength distributions as a function of orientation.

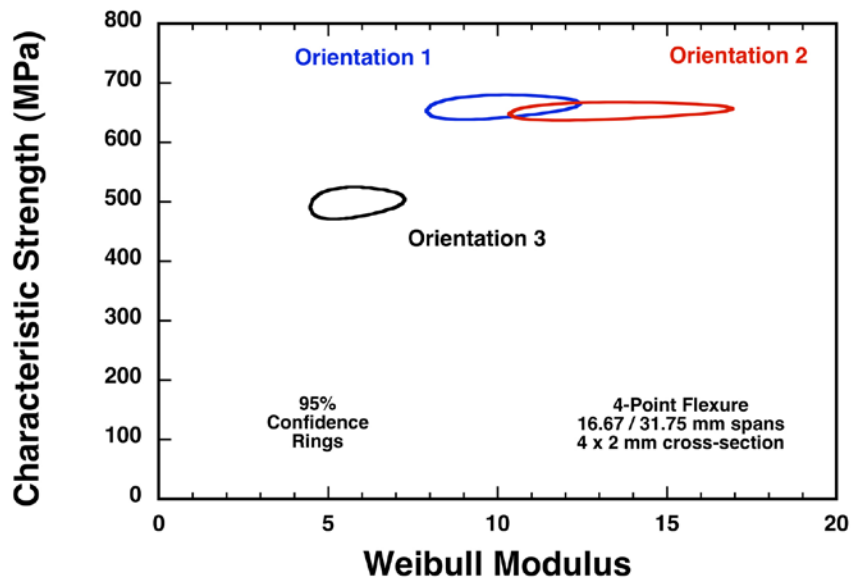


Figure 5. 95% Weibull confidence flexure strength rings as a function of orientation.

The calculated average fracture toughness,  $K_{Ic}$ , of each orientation is shown in Table III with a  $\pm$  value of one standard deviation. The  $K_{Ic}$  values of orientations 1 and 2 are equivalent, and agree with a previously calculated value for this material [5]. However, the value for orientation 3 is statistically significantly lower than that of the other two orientations and lower than the value previously calculated by more than 10%.

Table III. Average fracture toughness,  $K_{Ic}$ , as a function of orientation.

Orientation	Average $K_{Ic}$ ( $\text{MPa}\sqrt{\text{m}}$ )
1	$4.56 \pm 0.18$
2	$4.52 \pm 0.18$
3	$3.98 \pm 0.05$

*Contact Pressure Response (Indentation)*

Hardness averages were calculated with respect to orientation of specimen and alignment of Knoop indent. A schematic illustration of the parallel and perpendicular alignments on the test coupons is shown in Fig. 6, and the averages found for each combination of specimen orientation and indent alignment are shown in Fig. 7. There was no significant difference found with the hardness of 19.3 GPa falling within one standard deviation for each combination. This value is consistent with a previously measured Knoop hardness of this material [5].

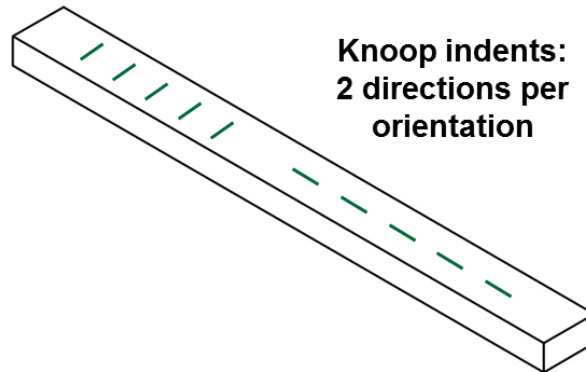


Figure 6. Schematic drawing depicting both perpendicular (left) and parallel (right) alignments of indent on a indentation test coupon.

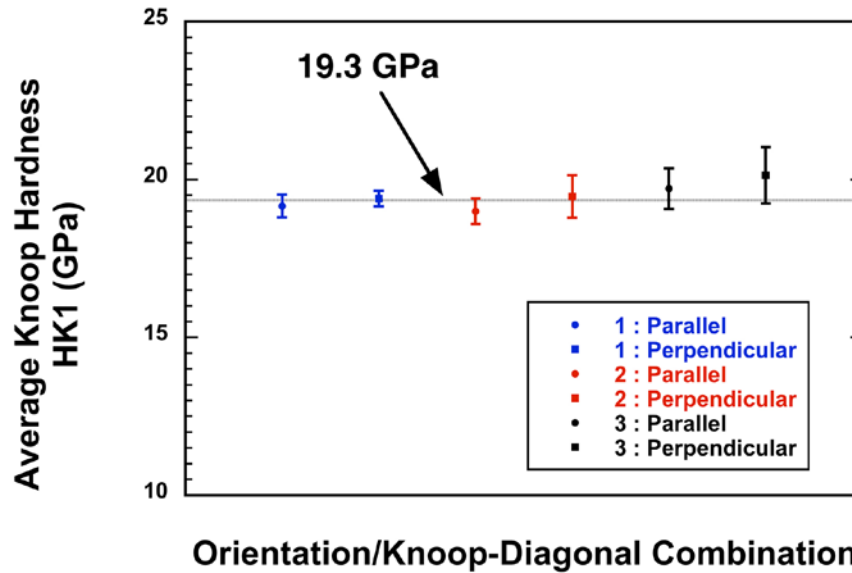


Figure 7. Average Knoop hardness, HK1, of six combinations of orientation and indent alignment. Alignment is with respect to each test coupon's long axis.

Examination of indent tips with SEM imaging showed that levels of cracking varied amongst orientation combinations. In combinations where cracks formed in the R-Z plane – both alignments in orientation 1, perpendicular in orientation 2 and parallel in orientation 3 – there was only mild to moderate cracking. Cracks that did extend from the tips of the indents were intergranular. Cracks that formed in the R-R plane, such as those that extended from the perpendicularly aligned Knoop indents of orientation 3 and parallel in orientation 2, were larger and had significant amounts of transgranular fracture. Such behavior corresponds with findings from the flexure strength and fracture toughness testing.

Averages for maximum spherical IDOP and residual indent depth were measured for each orientation. The resulting values – maximum IDOP and residual indent depth, respectively are shown in Fig. 8. These figures show that each orientation responded differently to the spherical indentation. This was unexpected as in both orientations 2 and 3 the indented face comes from an R-Z plane of the original block. In a homogeneous block, responses in these orientations would be identical. However, as only one coupon of each orientation was tested, it is difficult to determine whether this is a localized effect or the representativeness of their data. Despite this, the ability of spherical indentation to measure dissimilarity in these specimens suggests it may be effective at exploiting an effect that traditional Knoop indentation did not.

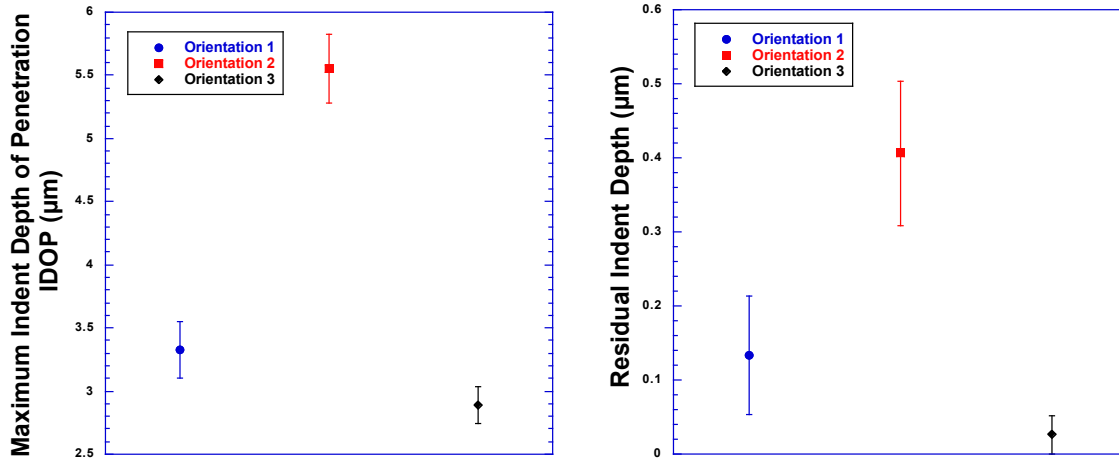


Figure 8. Spherical indentation maximum indent depth of penetration (left), and residual indent depth (right), respectively, as a function of orientation.

## CONCLUSIONS

Fracture processes were transversely isotropic in a 40-mm-thick tile of hot-pressed SiC. The flexure strength and fracture toughness were  $\sim 25\%$  and  $10\%$  lower, respectively, in the plane perpendicular to the pressing axis compared to the plane parallel to the pressing axis.

Knoop hardness was isotropic but the measured spherical indentation responses were different. The significance of the latter and its interpretation are not presently understood. More tests among more test coupons are needed to resolve that.

The effect of the amount of transverse isotropy of fracture on ballistic response is not known; however, it suggests that a dynamic, fracture-related process, such as spall, may be different in different directions. It would be worthwhile to examine this by challenging the assumption of isotropy in ballistic modeling of hot-pressed SiC.

## ACKNOWLEDGEMENTS

Research performed under Work For Others funded by U.S. Army Tank-Automotive Research, Development and Engineering Center, under contract DE-AC-00OR22725 with UT-Battelle, LLC.

The authors express sincere appreciation to A. Dolan, R. Rickert, and D. Templeton of the U.S. Army Research, Development and Engineering Command - Tank-Automotive and Armaments Command for sponsoring this work, ORNL's H. -T. Lin for the FE-SEM imaging, and ORNL's M. Ferber and R. Wiles for their review of this manuscript and helpful comments.

This submission was produced by a contractor of the United States Government under contract DE-AC05-00OR22725 with the United States Department of Energy. The United States Government retains, and the publisher, by accepting this submission for publication, acknowledges that the United States Government retains, a nonexclusive, paid-up, irrevocable, worldwide license to publish or reproduce the published form of this submission, or allow others to do so, for United States Government purposes.

This report was prepared as an account of work sponsored by an agency of the United States Government. Neither the United States Government nor an agency thereof, or any of their employees, makes any warranty, express or implied, or assumes legal liability or responsibility for the accuracy, completeness, or usefulness of any information, apparatus, product, or process disclosed, or represents that its use would not infringe privately owned rights. Reference herein to any specific commercial product, process, or service by trade name, trademark, manufacturer, or otherwise does not necessarily constitute or imply endorsement, recommendation, or favoring by the United States Government or any agency thereof. The views and opinions of authors expressed herein do not necessarily state or reflect those of the United States Government or any agency thereof.

## REFERENCES

- [1] F. F. Lange, "Relation Between Strength, Fracture Energy, and Microstructure of Hot-Pressed  $\text{Si}_3\text{N}_4$ ," *J. Am. Ceram. Soc.*, 56:518-522 (1973).
- [2] J. E. Weston, "Origin of Strength Anisotropy in Hot-Pressed Silicon Nitride," *J. Mater. Sci.*, 15:1568-1576 (1980).
- [3] T. Nagaoka, S. Kanzaki, Y. Yamaoka, "Mechanical Properties of Hot-Pressed Calcium Hexaluminate Ceramics," *J. Mater. Sci. Letters*, 9:219-221 (1990).
- [4] A. Takashi, T. Yasuhiro, Y. Eiichi, "Anisotropies and Mechanical Properties of Hot-Pressed  $\text{Al}_2\text{O}_3$  and SiC whisker/ $\text{Al}_2\text{O}_3$  Composites" *J. Mater. Res.*, 9:207-215 (1994).
- [5] A. A. Wereszczak, K. E. Johanns, and O. M. Jadaan, "Hertzian Ring Crack Initiation in Hot-Pressed Silicon Carbides," *J. Am. Ceram. Soc.*, 92:1788-1796 (2009).
- [6] "Standard Test Method for Flexural Strength of Advanced Ceramics at Ambient Temperature," ASTM C1161, Vol. 15.01, 2010, ASTM International, West Conshohocken, Pennsylvania.
- [7] "Standard Test Methods for Determination of Fracture Toughness of Advanced Ceramics at Ambient Temperature," ASTM C1421, Vol. 15.01, 2010, ASTM International, West Conshohocken, Pennsylvania.
- [8] "Standard Test Methods for Knoop Indentation Hardness of Advanced Ceramics," ASTM C1326, Vol. 15.01, 2008, ASTM International, West Conshohocken, Pennsylvania.
- [9] NIST Standard Reference Material for Knoop Hardness of Ceramics, SRM 2830.